Subtle Charge Balance Controls Surface-Nucleated Self-Assembly of Designed Biopolymers

Céline Charbonneau, J. Mieke Kleijn,* and Martien A. Cohen Stuart

Laboratory of Physical Chemistry and Colloid Science, Wageningen University, Dreijenplein 6, 6703 HB Wageningen, The Netherlands

ABSTRACT We report the surface-nucleated self-assembly into fibrils of a biosynthetic amino acid polymer synthesized by the yeast *Pichia pastoris*. This polymer has a block-like architecture, with a central silk-like block labeled S^H, responsible for the self-assembly into fibrils, and two collagen-like random coil end blocks (C) that colloidally stabilize the fibers in aqueous solution. The silk-like block contains histidine residues ($pK_a \approx 6$) that are positively charged in the low pH region, which hinders self-assembly. In aqueous solution, CS^HC self-assembles into fibers above a pH-dependent critical nucleation concentration C_c^b. Below C_c^b, where no self-assembly occurs in solution, fibril formation can be induced by a negatively charged surface (silica) in the pH range of 3.5—7. The density of the fibers at the surface and their length are controlled by a subtle balance in charge between the protein polymer and the silica surface, which is evidenced from the dependence on pH. With increasing number density of the fibers at the surface, their average length decreases. The results can be explained on the basis of a nucleation-and-growth mechanism: the surface density of fibers depends on the rate of nucleation, while their growth rate is limited by transport of proteins from solution. Screening of the charges on the surface and histidine units by adding NaCl influences the nucleation-and-growth process in a complicated fashion: at low pH, the growth is improved, while at high pH, the nucleation is limited. Under conditions where nucleation in the bulk solution is not possible, growth of the surface-nucleated fibers into the solution—away from the surface—can still occur.

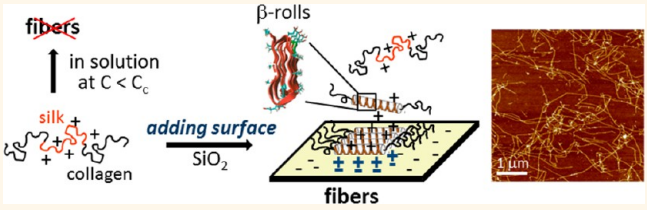

KEYWORDS: triblock protein polymers · protein fibers · silica surface · electrostatic interactions · nucleation-and-growth mechanism · surface-induced assembly

Many biopolymers, in particular, proteins, are well-known to form various nanostructures in solution such as nanowires, nanofibers, nanotubes, and vesicles.[1] In turn, nanofibers usually form hydrogels at high concentration, and the stimuli-responsive properties of these have generated a strong interest in medicine.[2] The process of nanofiber formation is usually kinetically controlled and involves a nucleation step. Often this is a homogeneous nucleation, but recently, several cases have been reported where fibril formation occurred on a surface rather than in solution. This has practical applications in industrial biosensors, in biotechnology, and in nanotechnology.[3,4]

Surface-mediated fibril formation has been reported for several oligopeptides (typically 20 amino acids long)[5−8] and for amyloid beta.[9−12] The surface attachment in these cases was by physisorption[6−9,12] on mica or pyrolytic graphite (HOPG) or also by chemisorption.[5,10,11] One report concerns nanofiber formation on mica by a silk-elastine-like polymer (71 kDa) carrying a short cationic end block.[13] Self-assembly most likely follows a nucleation-and-growth process that can take place either in solution[6−9,11,12] or directly on the surface by adsorption of individual molecules coming from solution.[5,10,13] In the former case (majority of surface-mediated fibril formation), "seeds" are preformed in solution which continue to grow after adsorption on the surface. It has been found that the morphologies of surface-induced fibers can be tuned by changing the concentration of proteins, the physicochemical properties of the surface, and environmental conditions such as temperature, pH, and ionic strength,[3,5,7,8,11,13,14] although a systematic variation of all these parameters has not been undertaken in the various cases. Fibril growth can also take place in an oriented, epitaxial fashion by using

* Address correspondence to mieke.kleijn@wur.nl.

Received for review November 8, 2013 and accepted February 26, 2014.

Published online February 26, 2014
10.1021/nn405799t

structured surfaces such as mica or highly oriented pyrolytic graphite.[6,7,15,16] It is, however, not fully clear what the prerequisites are for surface-induced self-assembly to occur. In ref 13, the fiber number density turned out to be dependent on ionic strength, and it was concluded from this that electrostatics plays an important role. However, no pH variation was undertaken which might have substantiated this claim. Clear evidence of surface-induced nucleation, and in particular how this depends on protein−surface interactions, has not been reported so far.

Here, we investigate the surface-induced self-assembly of a biosynthetic amino acid polymer ("protein polymer") on a negatively charged surface (silica). The polymer has been designed to have a block-like structure, composed of a central pH-sensitive silk-like block (S^H) flanked by two random-coil collagen-like blocks (C). The silk-like block has the amino acidic sequence $(GAGAGAGH)_{48}$, with G = glycine, A = alanine, and H = histidine. The associative behavior of CS^HC in solution[17−19] and the rheological properties of hydrogels that these protein polymers form at high concentration and high pH[20] have been studied elsewhere. It has been found that spontaneous self-assembly into fibers occurs by stacking of the silk-like blocks (uncharged at high pH), which most likely fold into β-rolls, stabilized by hydrogen bonds.[21,22] The stacking is driven by the hydrophobic nature of the surface of these folded domains. The collagen-like blocks are soluble at all pH values and form random coils, which provide the steric repulsion needed to prevent the aggregation of the sticky silk-like blocks.[23] It has been concluded from circular dichroism measurements that the folded state of the silk-like blocks appears when a block attaches to a growing fiber.[19]

The objective of this study is to demonstrate that fibril formation of CS^HC can occur in a concentration and pH range where self-assembly in solution does not happen, and that a necessary condition for this is the presence of a surface with which the silk-like block can have attractive electrostatic interactions. A negatively charged silica surface fulfills these requirements. We use AFM to investigate the number density and length of the surface-induced fibers as a function of pH, ionic strength, and protein polymer concentration.

RESULTS

We first consider fibril formation in solution. It has been previously reported that fibril formation of CS^HC in solution occurs at high pH where the histidine units in the silk-like blocks are uncharged.[19,20] Here, we extend this study to the pH range of 3−8 as this is the range where silica and the polymer have opposite charges, so that attractive electrostatic interactions with the surface are likely to occur. We first investigate whether there is a nucleation threshold, here defined as the lowest concentration for which we can still observe fibrils after a fixed time, for which we (arbitrarily) choose 24 h. To this end, solutions of various concentrations and pH are first incubated for 24 h. In order to observe fibrils in cases where these have formed, samples are prepared by immersing a piece of (untreated) silicon wafer into the solutions during a few minutes, at the end of the experimental time of 24 h. We indeed find that CS^HC, after a period over 24 h, self-assembles into fibrils over the entire pH range of 3−8, provided that the concentration exceeds a minimum value (threshold). This nucleation threshold, or critical concentration (C_c^b), corresponds to the concentration above which fibers are visible by AFM (*i.e.*, have a length >10 nm). Figure 1 presents C_c^b as a function of pH (in the absence of salt). C_c^b first decreases from ∼1.5 mg/mL at pH 3 to ∼0.17 mg/mL at pH 5 and remains constant beyond pH 5. We also find that fibrils, once formed, do not fall apart upon lowering the concentration, which implies that C_c^b is a kinetic parameter rather than an equilibrium value such as a critical association or micellization concentration. We return to the meaning of C_c^b in the Discussion section.

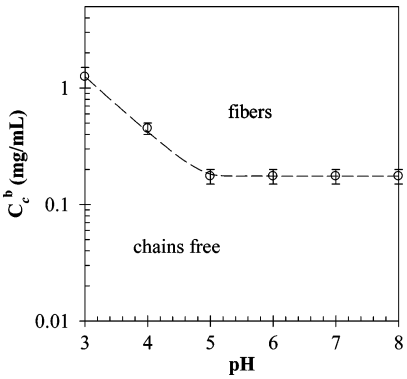

Figure 1. Critical concentration C_c^b of CS^HC *versus* pH for fibril formation in solution (no added NaCl). The dashed line is a guide for the eye. The error bars give at each pH the concentration interval between the highest concentration where no fibers were observed and the lowest concentration at which fibers were visible.

In the images of fibers, obtained after 24 h of incubation, we observe pH dependences, as can be seen in Figure 2. The length increases strongly with increasing pH from a few tens of nanometers at pH 4 to several micrometers (>5 μm) at pH 7. As expected, the width (∼20 nm) and the height (∼2 nm) of the fibers are the same over the entire pH range. This observation implies that pH does not influence the local structure of fibers but only its rate of formation. Hence, the mechanism which lies at the origin of the fibril formation, that is, folding and stacking of the S^H domains driven by hydrophobic interactions and hydrogen bonding,[21,22] is the same, whatever the pH. In addition, we observe that the fibers exhibit a broad length distribution, meaning that new fibrils nucleate continuously during the experiment.

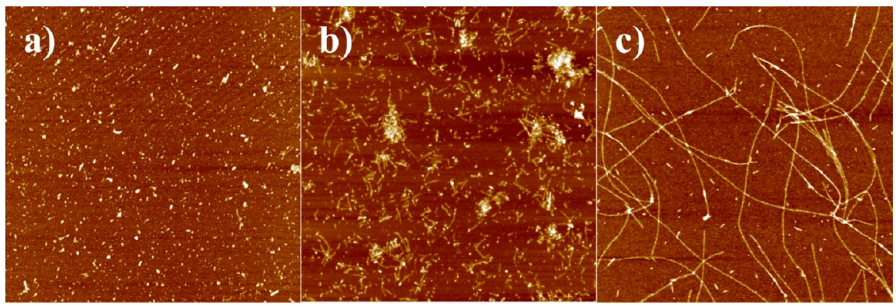

Figure 2. AFM images of fibers formed in solution at C = 0.50 mg/mL at (a) pH 4, (b) pH 5, and (c) pH 7 without NaCl. The images are 5 μm × 5 μm in size.

In the following, we will focus on the associative behavior of CS^HC in the presence of a negatively charged surface (silica). Since we want to particularly focus on the role of a surface, we concentrate on the range $C < C_c^b$, thereby excluding fibril formation in solution. In contrast to the previous experiment, we now incubate a piece of oxidized silicon from the beginning and analyze its surface after 24 h. We find that in a certain pH range fibrils are indeed formed at concentrations significantly lower than C_c^b, and that there is a new critical concentration, which we label C_c^s, below which fibril formation does not occur within the chosen time window. In Figure 3, we plot this C_c^s as a function of pH. For clarity, we also present the threshold concentration C_c^b for fibril formation in solution. We can clearly distinguish three regions. At the highest concentrations, protein polymers self-assemble into pH-sensitive fibers both in solution and likely also at the surface, while at the lowest concentrations, no self-assembly can be observed at all within the chosen time window of 24 h. At intermediary concentrations, fibril formation is observed, even though it cannot occur in solution; hence it has to be mediated by the (negatively charged) surface. This effect occurs in a narrow pH range between pH 3.5 and 7, with an optimum at pH ≈5.2 where C_c^s attains its lowest value. This distinct optimum suggests that electrostatic attraction between CS^HC and silica plays a role; we evaluate this hypothesis in the Discussion section. In the remainder of this section, we consider the structure (length, cross section) of the fibrils and how this depends on pH and ionic strength.

Formation of Fibers. Figure 4 shows AFM images of a silica surface after 15, 390, and 720 min of incubation in a solution of CS^HC, at a concentration C of 0.10 mg/mL and pH 6.2. After 15 min of incubation, short fibers of around 200 nm are already formed; they have a height of around 2 nm and a width of around 20 nm. This indicates that fibers start to grow on the surface without a substantial time lag. The average length of the fibers increases linearly with the square root of time (Figure 5), suggesting a diffusion-limited process. In the course of time, the length distribution widens, as indicated by the error bars (standard deviation) in Figure 5. Long fibers of around 1500−2000 nm are formed after 24 h of incubation.

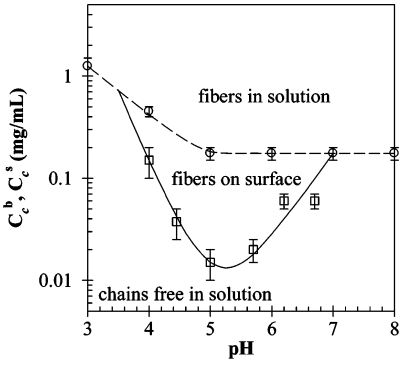

Figure 3. Critical concentrations C_c^b and C_c^s of CS^HC as a function of pH, both in solution (○) and on the negatively silica charged surface (□) (no added NaCl). The solid and dashed lines are guides for the eye. The meaning of the error bars is the same as in Figure 1.

We notice that the fibers exhibit a rather broad distribution in lengths and grow in random directions, suggesting that new fibers appear all the time during incubation. We can also see that they form neither branched structures nor bundles, which is similar to the fibril formation in solution. Martens *et al.*[18] considered the effect of the position of silk-like blocks along the protein polymer backbone on the structure of fibers, by comparing polymers with central silk-like blocks (CSC) and with silk-like end blocks (SCS). They found that bundles were seldom seen when the silk-like blocks were situated in the middle, whereas the presence of silk-like blocks at the end of chains sometimes led to bridging due to the insertion of silk-like blocks in two different fibers.

Finally, it is important to notice that fibers frequently cross; the height of the crossing points is around 4 nm (see Figure 6), which is twice the height of an individual fiber. This implies that fibers, in order to grow, do not have to be in contact with the silica over their entire length.

Effect of pH. Figure 7 shows AFM images of a silica surface after 24 h of incubation in salt-free solutions of CS^HC at C = 0.10 mg/mL and at six different pH values. At pH ≤ 4, surface-induced fibril formation does not

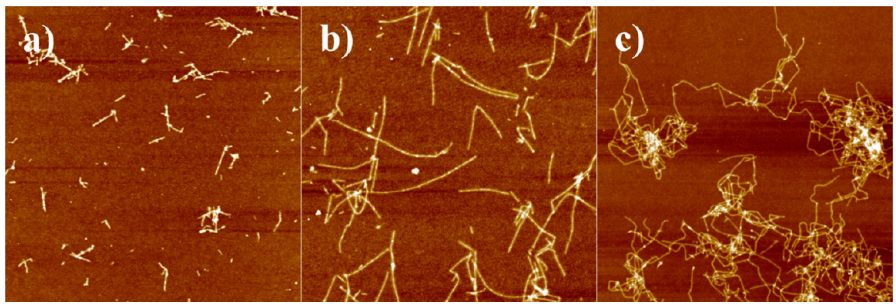

Figure 4. AFM images of a silica surface after (a) 15, (b) 390, and (c) 720 min of incubation in a solution at C = 0.10 mg/mL, at pH 6.2, and without NaCl. The images are 5 μm × 5 μm in size.

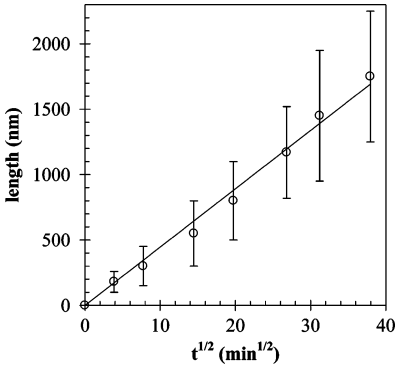

Figure 5. Evolution of the average length of fibers of CS^HC at the oxidized silicon surface as a function of square root of incubation time for C = 0.10 mg/mL, pH 6.2, no NaCl added. The solid line corresponds to a linear regression fit (slope = 44.6 nm/min$^{1/2}$).

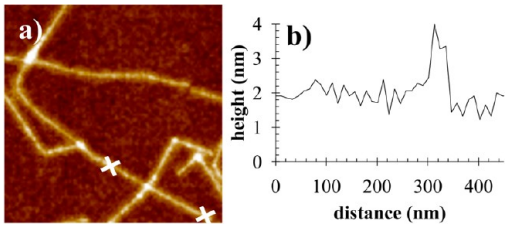

Figure 6. (a) AFM image showing the crossing of fibers. Incubation time 390 min, C = 0.10 mg/mL, pH 6.2, no NaCl added. The image is 1 μm × 1 μm in size, zoomed in from a 5 μm × 5 μm scan. (b) Height profile at a crossing point between two fibers measured between the white crosses in panel a.

occur. However between pH 4 and 7, fibers are formed on the negatively charged surface. Their average length is pH-dependent and plotted in Figure 8. In the range 4 < pH ≤ 5.7, the average length increases gradually with increasing pH (Figure 7a–c), then increases sharply from around 150 nm at pH 5.7 (d) to around 1500–2000 nm at pH 6.2, and then seems to drop strongly to around 450 nm at pH 6.7 (e). Over the same range, the number density of the fibers decreases strongly and continuously with increasing pH. The total grown fibril length, given by the product of fiber length and number density, increases with increasing pH (see the inset in Figure 8). At pH ≥ 7, no more fibers are observed on the surface. The fiber morphology, in terms of width (~20 nm) and height (~2 nm), is independent of the pH. Again, the fibers are oriented randomly and present a broad length distribution, for each pH.

Effect of Ionic Strength. We studied the effect of ionic strength on the surface-mediated fibril formation at two pH values, namely, 4 and 6.2. Figure 9 represents AFM images of a silica surface after 24 h of incubation in a solution at C = 0.10 mg/mL and in the presence of 0, 100, and 200 mM of NaCl. Increasing the salt concentration potentially affects all electrostatic interactions: protein–protein (repulsive) and protein–surface (attractive). Therefore, it has two opposite effects on the surface-mediated fibril formation. As we saw before, without added salt, no fibrils form at pH 4. This changes when salt is added: at pH 4 and 100 mM NaCl, many rather irregular clusters are formed, and at 200 mM NaCl, we find some clusters but also well-defined fibers of around 100 nm of length. At pH 6.2, fibrils form readily in salt-free samples. Perhaps surprisingly, few and short fibers of only a few hundreds of nanometers in length are observed when salt was present; their number density is somewhat higher at 200 mM NaCl than at 100 mM NaCl.

Effect of the Protein Polymer Concentration. Figure 10 shows AFM images of a silica surface after 24 h of incubation in salt-free solutions of CS^HC at pH 6.2 and at four different protein polymer concentrations: C = 0.05, 0.07, 0.10, and 0.15 mg/mL. The number density of fibers decreases with decreasing protein polymer concentration, and below a critical concentration (between 0.05 and 0.07 mg/mL), the surface-mediated fibril formation is no longer observed. The average length of fibers increases with decreasing concentration, from around 500 nm at C = 0.15 mg/mL to around 1500–2000 nm at C = 0.10 and 0.07 mg/mL. A similar trend was observed for other pH values.

DISCUSSION

We demonstrated that CS^HC forms fibers in solution above a pH-dependent critical concentration C_c^b (Figure 1) and found that these fibers are stable upon dilution. Hence, C_c^b cannot be regarded as an equilibrium critical concentration (like, *e.g.*, a critical

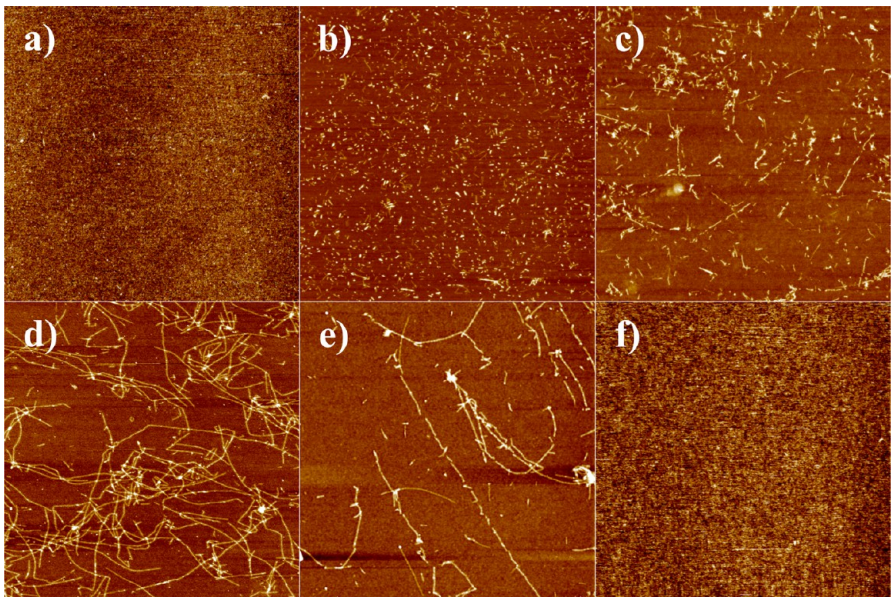

Figure 7. AFM images of a silica surface after 24 h of incubation in solutions of $CS^{H}C$ at $C = 0.10$ mg/mL and in the absence of NaCl for (a) pH 4, (b) pH 5, (c) pH 5.7, (d) pH 6.2, (e) pH 6.7, and (f) pH 7. The images are 5 μm $\times$ 5 μm in size.

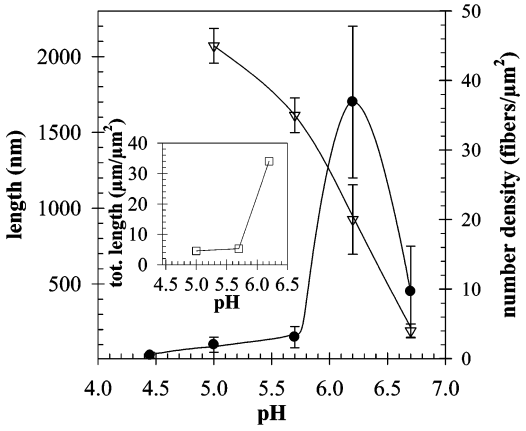

Figure 8. Average length (●) and number density (▽) of fibers as a function of pH for $CS^{H}C$ at $C = 0.10$ mg/mL (no added NaCl) after 24 h of incubation. The inset corresponds to the evolution of the total fibril length as a function of pH. The solid lines are guides for the eye. The error bars correspond to the lowest and highest length and number density.

micellization concentration) but is a kinetic property. Since the formation of fibers must start somehow, C_c^b should most likely be interpreted as a threshold for homogeneous nucleation. Comparable molecules, like $CS^{E}C$ which has a glutamic acid residue instead of a histidine, also form very similar fibrils by a nucleation-and-growth process.[19] There are of course differences: $CS^{E}C$ fibril formation requires an acidic medium (pH $\leq$ 5), and nucleation does not seem to occur from dissolved molecules (true homogeneous nucleation) but from a fixed number of nuclei per unit weight of dry sample (pseudo-heterogeneous nucleation), so that these fibrils tend to be monodisperse. In our case, we have seen that for self-assembly in bulk solution the nucleation threshold concentration C_c^b depends on pH, increasing for pH < 5, where the polymer progressively acquires positive charge by protonation of the histidine residues ($pK_a \approx 6$).[24] This suggests that there is an electrostatic contribution to the nucleation barrier. In the presence of a silica surface, we find in the pH range of 3−7 another critical concentration for fibril formation, C_c^s, which is lower than C_c^b by a factor that has a maximum around pH 5.2 (Figure 3). Since we know that fibril formation in solution cannot occur below C_c^b, this immediately implies that fibril formation is induced by the (negatively charged) silica surface. Hence the surface enhances at least the rate of nucleation, most likely by electrostatically driving the adsorption of protein polymers. We verified that the collagen-like blocks have no affinity for the silica surface (results not shown). The accumulated molecules at the surface seem to form nuclei more easily than the free molecules in solution, possibly because screening lowers the electrostatic repulsion between the molecules.

From Figure 4 alone, it is not possible to decide whether the growth of nuclei generated at the surface is possible into solution at these low concentrations ($C_c^s < C < C_c^b$), or that fibrils only grow in close contact with the surface. However, as we can see from various AFM images (*e.g.*, in Figure 6), fibrils can form crossings which necessarily means that at least part of the growth has not taken place in contact with the surface. Hence, we infer that the surface primarily affects the nucleation rate, and that growth can take place in solution, too.

The fact that surface-induced nucleation takes place in a limited pH range strongly suggests that an electrostatic mechanism is operative here. Upon increasing the pH from 3 to 7, the surface charge density of silica, σ^-, increases from a very low to a substantial value,[25]

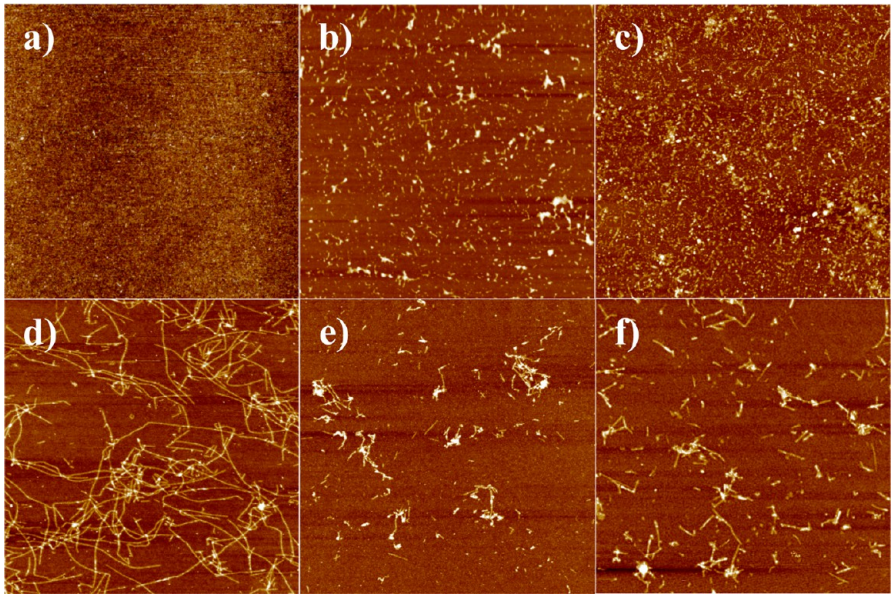

Figure 9. AFM images of a silica surface after 24 h of incubation in solutions of CS^HC at C = 0.10 mg/mL; (a−c) at pH 4 and (a) 0 mM, (b) 100 mM, and (c) 200 mM NaCl; (d−f) at pH 6.2 and (d) 0 mM, (e) 100 mM, and (f) 200 mM NaCl. The images are 5 μm × 5 μm in size.

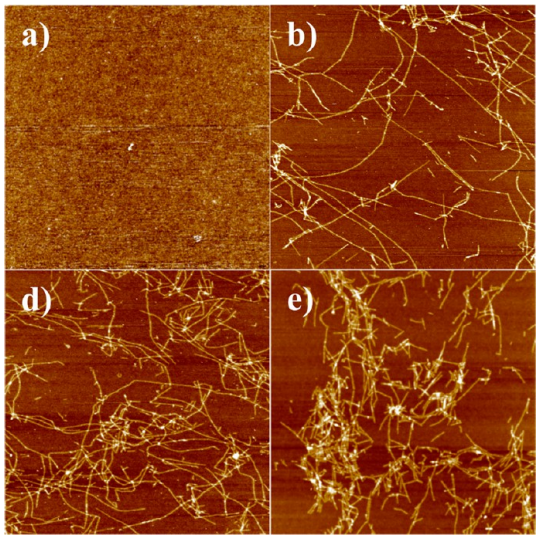

Figure 10. AFM images of a silica surface after 24 h of incubation in a solution of CS^HC, at pH 6.2, and a protein polymer concentration C of (a) 0.05, (b) 0.07, (c) 0.10, and (d) 0.15 mg/mL, in the absence of NaCl. The images are 5 μm × 5 μm in size.

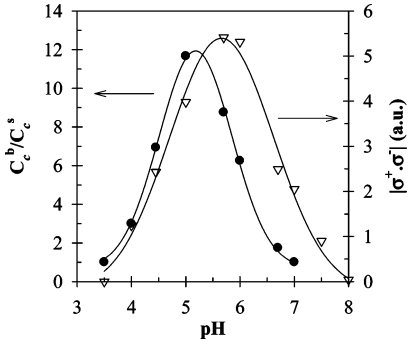

Figure 11. Correlation between the ratio of the critical concentrations for fibril formation in solution and in the presence of a silica surface C_c^b/C_c^s (●) and the electrostatic attraction, expressed by the product of the charge densities of CS^HC and silica, $|\sigma^+\sigma^-|$ (▽) as a function of pH. The solid lines are guides for the eye. Both curves are remarkably similar, from which we infer that C_c^b/C_c^s is clearly correlated to the strength of electrostatic attraction. It should be realized that the charge densities have been calculated for free silica and histidine, whereas in reality, they interact, which may lead to modest shifts on the pH axis and tend to strengthen the interaction.

whereas the charge on the silk-like block S^H decreases due to deprotonation of the histidine units. Hence the electrostatic attraction, which essentially follows the product of the respective charge densities $\sigma^+\sigma^-$, will have a maximum somewhere halfway in the range 3 < pH < 7. To substantiate the idea that enhancement of the nucleation rate (expressed by the ratio C_c^b/C_c^s) correlates with electrostatic attraction, we plotted in Figure 11 both C_c^b/C_c^s and $|\sigma^+\sigma^-|$ as a function of pH. Data for the surface charge density of silica have been obtained from ref 25, and the charge density of the protein polymer as a function of pH has been calculated from the pK_a of the histidine residues (see Experimental Section).

The length and number density of the fibers (at constant protein polymer concentration) turns out to be strongly dependent on both pH and salt concentration (Figures 7−9). In the absence of salt and over the pH range of 4−7, the number density drops from a high value at low pH to virtually zero around pH 7. The average length has a maximum at around pH 6.2, and then seems to decrease steeply upon increasing the pH; however, we should realize that at low density the length statistics are relatively poor. The fact that the total growth of the fibers decreases with decreasing pH

(inset of Figure 8) is in line with the growth dynamics being controlled by an energy barrier that depends on the repulsive intermolecular interactions between histidine units in the silk-like blocks.

Screening of the charged surface and histidine units, by adding NaCl, has a strong effect on both protein−surface attraction and protein−protein repulsion. At pH 4, screening of intermolecular repulsive interactions decreases the energy barrier, thus favoring the growth of fibers. At pH 6, screening of the low charge density of proteins substantially weakens protein−surface attraction and, consequently, lowers the nucleation rate.

CONCLUSION

We have demonstrated that the self-assembly of CS^HC protein polymers can be induced by a negatively charged surface (silica) under conditions where fibril formation in solution does not take place (*i.e.*, at CS^HC concentrations below the critical concentration C_c^b). The ratio between C_c^b and the critical concentration for fibril formation at the surface, C_c^s, correlates strongly with the product of the pH-dependent charge densities of the protein polymer and the silica surface, $\sigma^+\sigma^-$, indicating that the nucleation is controlled by a subtle balance in charge between histidine units inside the silk-like blocks of CS^HC proteins and the negatively charged surface. Decreasing repulsive interactions between the positively charged histidine units inside the silk-like blocks, by increasing the pH, favors the elongation of fibers but limits nucleation. Screening the charges by adding NaCl favors the growth of fibers at low pH (intermolecular repulsive interactions decreased) but limits the nucleation at high pH (protein−surface attractions screened).

Once nuclei have been generated at the negatively charged surface, at $C_c^s < C < C_c^b$, fibril growth of CS^HC occurs not only along the surface but also from the surface-bound nuclei into the solution. This phenomenon opens the possibility to grow fibers by heterogeneous nucleation from silica nanoparticles. This may lead not only to better fibril length control (through the surface area to solution volume ratio) but also to novel hybrid silica−protein polymer networks.

EXPERIMENTAL SECTION

Materials. CS^HC was biosynthesized following the procedure described by Li *et al.*[17] It is a strictly monodisperse compound with a molar mass of approximately 65 kDa and a well-defined amino acid sequence. The central silk-like block (S^H) has the sequence (Gly-Ala-Gly-Ala-Gly-Ala-Gly-His) repeated 48 times. The collagen-like blocks have an amino acid composition close to that of natural collagen; that is, they are rich in hydrophilic amino acids but have an irregular, scrambled sequence.[20] As a result, they tend to form random coils, independently of pH and temperature. Hydrochloric acid (0.1 M, Merck), sodium hydroxide (0.1 M, Merck), and sodium chloride (Aldrich, >99%) were used as received. Water was demineralized using a Barnstead Easypure UV apparatus and had a typical resistance of 18.3 MΩ/cm. Silicon wafers were treated as described below.

Surface Preparation. A silicon wafer was oxidized by heating in an oven at 1000 °C for 2 h. Once oxidized, the plate was cut into small pieces. These were washed in ethanol for about 15 min under sonication, then rinsed with demineralized water and ethanol before being dried under a nitrogen stream. Just before use, the surfaces were cleaned a last time in a plasma oven for 10 min.

Solution Preparation. Every solution was prepared separately using the following procedure. CS^HC was initially dissolved in demineralized water containing 10^{-2} M of hydrochloric acid and homogenized by vigorous stirring for 1 h. The solutions were then filtered through 0.2 μm pore size polyethersulfone filters in order to remove dust and larger aggregates. Finally, the ionic strength and the pH of the solutions were adjusted by adding required (small) amounts of sodium chloride and sodium hydroxide.

Atomic Force Microscopy Imaging. AFM analyses were performed in air on a Nanoscope V multimode AFM (Bruker) in PeakForce tapping mode using ScanAsyst. Silicon nitride cantilevers with a nominal spring constant of 0.35 N/m (NP-10, Bruker) and a typical tip radius of 10 nm were used for all measurements. To obtain the best imaging quality, the scan rate was set to 1 Hz. All AFM images were taken of dried samples. For that, wafers were quickly rinsed with a small amount of demineralized water to remove residual salt on the surface and then quickly dried under a nitrogen stream. The length of fibers was determined from around 100 fibers randomly measured on three different images of 5 μm × 5 μm in size, and the number was determined from six images of 2 μm × 2 μm in size.

Charge Density on CS^HC and Silica Wafers. Due to the presence of 48 positively charged histidine units along the silk-like blocks, CS^HC peptides have a pH-dependent charge. The charge density of the peptides (σ^+) is proportional to the degree of protonation of the histidine residues (α), and this has been calculated as follows:

$$\alpha = \frac{10^{pK_a - pH}}{1 + 10^{pK_a - pH}} \quad (1)$$

where $pK_a \approx 6$ as reported in the literature.[24] The charge density of silica (σ^-) was determined from potentiometric acid/base titration of a dispersion of silica nanoparticles.[25]

Conflict of Interest: The authors declare no competing financial interest.

Acknowledgment. This research was funded by the European Research Council through Advanced Grant 267 254 "Biomate". The CS^HC protein was kindly provided by L.H. Beun and F.A. de Wolf.

REFERENCES AND NOTES

1. Zhang, S. G. Fabrication of Novel Biomaterials through Molecular Self-Assembly. *Nat. Biotechnol.* **2003**, *21*, 1171–1178.
2. Kopecek, J.; Yang, J. Y. Smart Self-Assembled Hybrid Hydrogel Biomaterials. *Angew. Chem., Int. Ed.* **2012**, *51*, 7396–7417.
3. Zhang, Y.; Wu, C.; Guo, S.; Zhang, J. Interactions of Graphene and Graphene Oxide with Proteins and Peptides. *Nanotechnol. Rev.* **2013**, *2*, 27–45.
4. Scheibel, T.; Parthasarathy, R.; Sawicki, G.; Lin, X. M.; Jaeger, H.; Lindquist, S. L. Conducting Nanowires Built by Controlled Self-Assembly of Amyloid Fibers and Selective Metal Deposition. *Proc. Natl. Acad. Sci. U.S.A.* **2003**, *100*, 4527–4532.

5. Ku, S. H.; Park, C. B. Highly Accelerated Self-Assembly and Fibrillation of Prion Peptides on Solid Surfaces. *Langmuir* **2008**, *24*, 13822–13827.
6. Whitehouse, C.; Fang, J. Y.; Aggeli, A.; Bell, M.; Brydson, R.; Fishwick, C. W. G.; Henderson, J. R.; Knobler, C. M.; Owens, R. W.; Thomson, N. H.; *et al.* Adsorption and Self-Assembly of Peptides on Mica Substrates. *Angew. Chem., Int. Ed.* **2005**, *44*, 1965–1968.
7. Yang, H.; Fung, S. Y.; Pritzker, M.; Chen, P. Modification of Hydrophilic and Hydrophobic Surfaces Using an Ionic-Complementary Peptide. *PLoS One* **2007**, *2*, e1325.
8. Yang, H.; Fung, S. Y.; Pritzker, M.; Chen, P. Surface-Assisted Assembly of an Ionic-Complementary Peptide: Controllable Growth of Nanofibers. *J. Am. Chem. Soc.* **2007**, *129*, 12200–12210.
9. Blackley, H. K. L.; Sanders, G. H. W.; Davies, M. C.; Roberts, C. J.; Tendler, S. J. B.; Wilkinson, M. J. *In-Situ* Atomic Force Microscopy Study of β-Amyloid Fibrillization. *J. Mol. Biol.* **2000**, *298*, 833–840.
10. McMasters, M. J.; Hammer, R. P.; McCarley, R. L. Surface-Induced Aggregation of Beta Amyloid Peptide by ω-Substituted Alkanethiol Monolayers Supported on Gold. *Langmuir* **2005**, *21*, 4464–4470.
11. Moores, B.; Drolle, E.; Attwood, S. J.; Simons, J.; Leonenko, Z. Effect of Surfaces on Amyloid Fibril Formation. *PLoS One* **2011**, *6*, e25954.
12. Zhu, M.; Souillac, P. O.; Ionescu-Zanetti, C.; Carter, S. A.; Fink, A. L. Surface-Catalyzed Amyloid Fibril Formation. *J. Biol. Chem.* **2002**, *277*, 50914–50922.
13. Hwang, W.; Kim, B. H.; Dandu, R.; Cappello, J.; Ghandehari, H.; Seog, J. Surface Induced Nanofiber Growth by Self-Assembly of a Silk-Elastin-like Protein Polymer. *Langmuir* **2009**, *25*, 12682–12686.
14. Nayak, A.; Dutta, A. K.; Belfort, G. Surface-Enhanced Nucleation of Insulin Amyloid Fibrillation. *Biochem. Biophys. Res. Commun.* **2008**, *369*, 303–307.
15. Prokhorov, V. V.; Klinov, D. V.; Chinarev, A. A.; Tuzikov, A. B.; Gorokhova, I. V.; Bovin, N. V. High-Resolution Atomic Force Microscopy Study of Hexaglycylamide Epitaxial Structures on Graphite. *Langmuir* **2011**, *27*, 5879–5890.
16. Karsai, A.; Murvai, U.; Soos, K.; Penke, B.; Kellermayer, M. S. Z. Oriented Epitaxial Growth of Amyloid Fibrils of the N27C Mutant Beta 25−35 Peptide. *Eur. Biophys. J.* **2008**, *37*, 1133–1137.
17. Li, F.; Martens, A. A.; Aslund, A.; Konradsson, P.; de Wolf, F. A.; Cohen Stuart, M. A.; Sudholter, E. J. R.; Marcelis, A. T. M.; Leermakers, F. A. M. Formation of Nanotapes by Co-assembly of Triblock Peptide Copolymers and Polythiophenes in Aqueous Solution. *Soft Matter* **2009**, *5*, 1668–1673.
18. Martens, A. A.; Portale, G.; Werten, M. W. T.; de Vries, R. J.; Eggink, G.; Cohen Stuart, M. A.; de Wolf, F. A. Triblock Protein Copolymers Forming Supramolecular Nanotapes and pH-Responsive Gels. *Macromolecules* **2009**, *42*, 1002–1009.
19. Beun, L. H.; Beaudoux, X. J.; Kleijn, J. M.; de Wolf, F. A.; Cohen Stuart, M. A. Self-Assembly of Silk-Collagen-like Triblock Copolymers Resembles a Supramolecular Living Polymerization. *ACS Nano* **2012**, *6*, 133–140.
20. Golinska, M. D.; Włodarczyk-Biegun, M. K.; Werten, M. W. T.; Cohen Stuart, M. A.; de Wolf, F. A.; de Vries, R. J. Dilute Self-Healing Hydrogels of Silk-Collagen-like Block Copolypeptides at Neutral pH. *Biomacromolecules* **2014**, 10.1021/bm401682n.
21. Schor, M.; Bolhuis, P. G. The Self-Assembly Mechanism of Fibril-Forming Silk-Based Block Copolymers. *Phys. Chem. Chem. Phys.* **2011**, *13*, 10457–10467.
22. Schor, M.; Martens, A. A.; de Wolf, F. A.; Cohen Stuart, M. A.; Bolhuis, P. G. Prediction of Solvent Dependent Beta-Roll Formation of a Self-Assembling Silk-like Protein Domain. *Soft Matter* **2009**, *5*, 2658–2665.
23. Werten, M. W. T.; Wisselink, W. H.; van den Bosch, T. J. J.; de Bruin, E. C.; de Wolf, F. A. Secreted Production of a Custom-Designed, Highly Hydrophilic Gelatin in *Pichia pastoris*. *Protein Eng.* **2001**, *14*, 447–454.
24. Sachs, D. H.; Schechter, A. N.; Cohen, J. S. Nuclear Magnetic Resonance Titration Curves of Histidine Ring Protons. *J. Biol. Chem.* **1971**, *216*, 6576–6580.
25. Goveia, D.; Pinheiro, J. P.; Milkova, V.; Rosa, A. H.; van Leeuwen, H. P. Dynamics and Heterogeneity of Pb(II) Binding by SiO_2 Nanoparticles in Aqueous Dispersion. *Langmuir* **2011**, *27*, 7877–7883.